doi:10.3788/gzxb20154410.1022002

焦距递减的多聚焦人工复眼研究

罗家赛,郭永彩,王欣

(重庆大学 光电学院 光电技术与系统教育部重点实验室,重庆 400044)

摘 要:为了满足轻量化、微型化和大视场的要求,提出了一种焦距递减的多聚焦人工复眼,子眼以同心圆排布,同一同心圆上的子眼具有相同的焦距,从内到外焦距递减.采用光刻胶回流法制作该曲面人工复眼,通过光刻胶的用量与掩膜的设计将每个子眼的焦距控制在一个特定的范围,从而使所有的子眼能在同一平面聚焦.为了防止微透镜图形的破坏,采用了负压成型技术,制作了聚二甲基硅氧烷腔室用以在注胶时排除异物与空气.透镜材料 Norland81 具有良好的光学性能,且曝光时间比 Norland61 要快 3 至 5 倍.利用 ZEMAX 建立复眼模型并进行了模拟仿真,光线追迹结果表明该模型即使在大视场下也能获得清晰像点.

关键词:应用光学;复眼;光刻胶回流法;微透镜阵列;多通道成像;微光学器件;光刻胶加工;大视场;光学设计与制造

中图分类号:Q692; TH74; TN202 **文献标识码**:A **文章编号**:1004-4213(2015)10-1022002-6

Development of a Multi-focusing Artificial Compound Eye With Decreasing Focal Length

LUO Jia-sai, GUO Yong-cai, WANG Xin

(*Key Laboratory of Optoelectronic Technology and Systems of Ministry of Education of China, Chongqing University, Chongqing*, 400044, *China*)

Abstract: In order to meet the demand of lightweight, miniaturization, large fields of view, a multi-focusing artificial-compound-eye with a gradually decreasing focal length was proposed. The ommatidia were arranged in the form of concentric circles, and each one owned the same focal length in the same circle. The artificial-compound-eye was fabricated by the photoresist reflow method. Each ommatidium had a specific focal length within a small interval through the calculation of dosage of photoresist, so that all the ommatidia could focus on the same plane. As for the manufacturing process, negative pressure was applied to solve microlens deformation problems, and Polydimethylsiloxane coelomic compartment was used for injecting optical adhesives without any impurities. In addition, Norland81 as the moulding material has similar qualities to the previous one, yet it can be cured 3 to 5 times faster. The simulation model was established by ZEMAX, and the result of ray-tracing shown that a clear image point could be obtained even under large field of view.

Key words: Applied optics; Compound eye; Photoresist reflow; Microlens array; Multiple imaging; Micro-optical devices; photoresist fabrication; Large field of view; Optical design and fabrication

OCIS Codes: 220.0220; 220.4000; 230.3990; 110.4190

Foundation item: The Specialized Research Fund for the Doctoral Program of Higher Education of China (No. 20130191110021)

First author: LUO Jia-sai (1990—), male, Ph. D. candidate, mainly focuses on micro—optical design and fabrication technology. Email: luojiasai@vip.qq.com

Supervisor(Contact author): GUO Yong-cai (1962—), female, professor, Ph. D. degree, mainly focuses on optical measurement, image processing and pattern recognition. Email:ycguo@cqu.edu.com

Received: May 19, 2015; **Accepted**: Sep. 8, 2015

0 Introduction

In nature, compound eyes have outstanding optical properties including large Field of View (FOV), compact structure, high dynamic sensitivity and so on. As a branch of bionics, the Artificial Compound Eye (ACE) research process is mainly divided into three parts: abstract biology model, the mathematical model, complete optical system. Since the 1990s, a large number of compound eye structures appeared[1-8]. Despite considerable efforts, all those structures were manufactured on a planar substrate on account of the limitation of the machining technology at that time. Scholars devoted themselves to improve the imaging quality through developing a new structure, such as Jacques's artificial Apposition Compound eye Objective (APCO)[4] and Tanida. J's thin Observation Module by Bound Optics (TOMBO)[3].

The researchers gradually focus on the curved ACE due to the low resolution, small FOV and blind area of planar ACE in recent years. However, a separate 3d ACE can't imaging on the planar optical sensors on account of its curved focal plane. To steer the focal plane onto a commercial planar photoreceptor, numerous Optical Relay Devices (ORD) had been designed. Many of them use optical fiber bundles as ORD, part of them design a self-aligned waveguide, some others make use of field array to improve edge imaging quality, increase the FOV, and correct the off-axis light[9-13]. Thus, both of them are either bulky or hard to manufacture. Also the cost of these structures will be expensive.

Some researchers have improved the microlens array to gain a planar focal plane. Di Si et. al have presented a single-layer spherical compound eye imaging system[14]. Ki-Hun et al designed a ACE with fractal zone plate arrays[15]. It's worth mentioning that Dario et. al have created a micro-opto-electromechanical ACE consist of a microlens array, a neuromorphic photodetector array, and a flexible printed circuit board that are stacked, cut, and curved to produce a mechanically flexible imager[16]. Otherwise, more and more related imaging algorithm appeared with respect to image mosaic[17-18], the moving target tracking[19], and so on.

This paper present a multi-focusing ACE with a gradually decreasing focal length. Every aperture has been calculated accurately and simulated using Zemax. The planar array was manufactured though the photoresist reflow and the curved was fabricated by a manufacturing process based on the pneumatic auxiliary micro-replication of polymer elastomer with a Polydimethylsiloxane (PDMS) coelomic compartment. The selection of moulding material Norland81 protected related photolithography equipment. Zemax was used to simulate the optical property of this ACE.

1 Design and simulation

1.1 Design of the multi-focusing ACE

This study designed a novel curved ACE with a multi-focusing microlens array. In order to make it smaller and more compact, the ommatidia were arranged in the form of concentric circles as shown in Fig. 1. Every ommatidium owns the same focal length in the same circle with a decreasing trend from the inside to the outside. Each ommatidium was given a specific focal length through the calculation of dosage of photoresist to make all the ommatidia focused on the same planar plane.

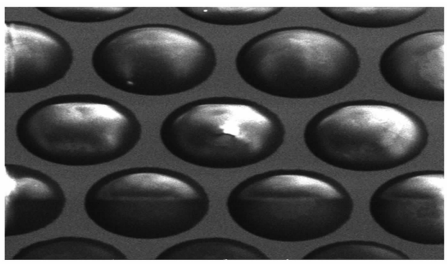

Fig. 1 The arrangement of multi-focusing ACE under the scanning electron microscope

1.2 Calculation of the lens parameters

Here, in order to calculate the geometry parameters of the multi-focusing ACE model, these significant parameters were defined in Fig. 2. The focal points of these microlens are desired to be located on the planar CCD plane and all optical axis get through the centre of sphere of the substrate. Therefore, parameters described above must satisfy the following equation[20]

$$l_n = R - \frac{R - l_0}{\cos(n\alpha_0 + \Delta\alpha_n)} \tag{1}$$

where, $\Delta\alpha_n = \frac{1}{2}(d_n - d_{n-2})/2$.

The formula of mirror grinding is known as follows

$$\frac{1}{f_n} = (n_0 - 1)\left(\frac{1}{r_n} - \frac{1}{R}\right) \tag{2}$$

For $f_n = l_n$

$$r_n = \frac{(n_0 - 1) f_n R}{R + (n_0 - 1) f_n} = \frac{(n_0 - 1) l_n R}{R + (n_0 - 1) l_n} \tag{3}$$

Combining with the ommatidium structure in Fig. 2, it can be obtained that

$$h_n = r_n(1 - \cos\theta) \tag{4}$$

$$d_n = 2r_n \sin\theta \tag{5}$$

It can be deduced from Eqs. (2)~(5) that we can control the dosage of photoresist and bottom radius of each ommatidium to control its focal length. Combining

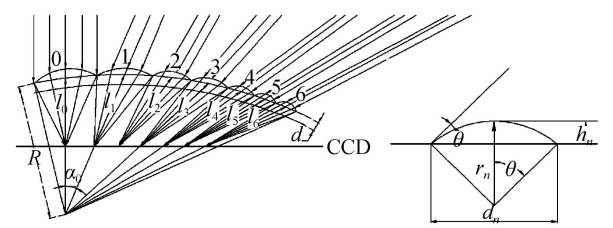

Fig. 2 The schematic diagram of multi-focusing ACE and ommidium

with the related formula of sphere and globoidal, researchers concluded the computational formula among the thickness of photoresist H, the focal length of microlens f and the thickness of microlens h in manufacturing process design.

$$r=\frac{d^2+4h^2}{8h}=\frac{(n_0-1)fR}{R+(n_0-1)f} \tag{6}$$

$$H\geqslant\frac{k^2}{2}h+\frac{2}{3D^2}h^2 \tag{7}$$

where, f, D and R are the regional parameters on account of the establishment of the initial model. Then r and h can be solved through Eq. (6). Finally, the dosage of photoresist can be calculated with the determination of H in Eq. (7), where $k\approx0.8$.

However, it brought in the deformation problem during curved surface forming, and the deformation rates of microlens on the same concentric circles remain equal. The diameter on different latitude increases by 9.45% to 10.56%[21]. Compensating the deformation should be the coming work.

1.3 Simulation of the multi-focusing ACE

The 3D model had been designed to simulate the optical properties in Zemax. Zemax can be implemented in the design of optical system modeling, analysis, and other auxiliary functions. Zemax is simple and easy to use, and it can realize interactive design with just a little practice. However, a cogent traditional evaluation indicator can't be acquired on account of those numerous separate ommatidium will affect the light distribution on an optical receiver. Therefore, we prefer to analyze the imaging capability of an individual ommatidium.

The model consist of a curved substrate and 35 ommatidia. All those ommatidia were arranged in the form of concentric circles on the substrate as shown in Fig. 3. Each ommatidium was designed a specific focal

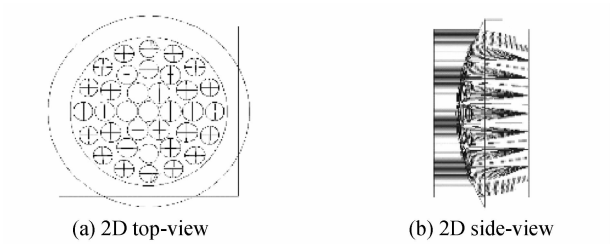

(a) 2D top-view (b) 2D side-view

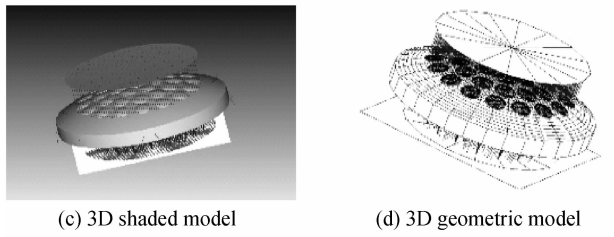

(c) 3D shaded model (d) 3D geometric model

Fig. 3 The schematic diagram of simulation model

length according to the location on the substrate. The spacing between each two ommatidia is within the scope of 20～40 μm and the bottom diameter changes among 200～400 μm.

Here, researchers simulated the imaging result under different FOV in Fig. 4. X axis and Y axis correspond to the vertical and horizontal FOV respectively in the simulation. With the angel of the incident light on the Y axis increasing, there's always one ommatidium imaging perfectly on the image plane, and the quality of those previous became more and more blurred.

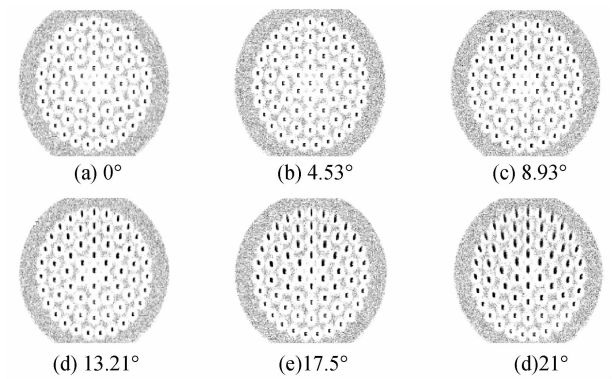

(a) 0° (b) 4.53° (c) 8.93°

(d) 13.21° (e)17.5° (d)21°

Fig. 4 The imaging result of the multi-focusing ACE

Each ommatidium can imaging clearly in a certain range of FOV. Researchers verified it by ray tracing for each ommatidium separately. Those ommatidium have a certain slope due to the arrangement on a spherical substrate. Certain one can receive normal incidence light with the related incident angle. That is to say, one ommatidium can get clearest Image Point (IP) when the incident angle equals the angle of inclination as shown in Fig. 5. Certainly, the effect of the central one was still better than others on account of the curved substrate.

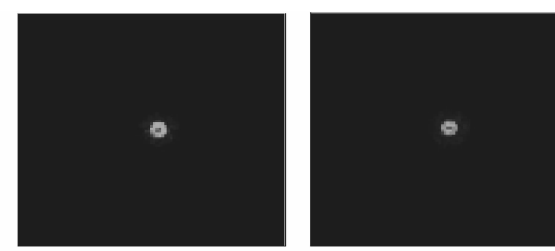

(a)The IP of first ring (b)The IP of second ring

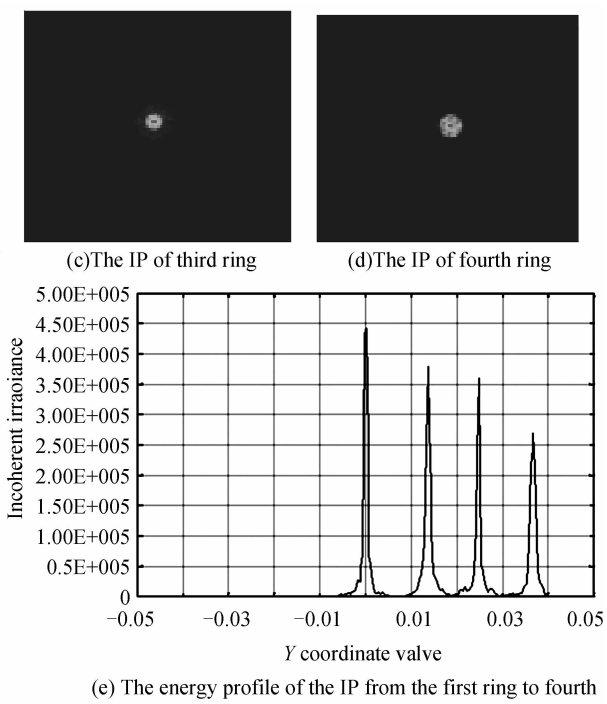

Fig. 5 The imaging result of the ommatidium with the related incident angle

However, serious coma appeared under large incident angle as shown in Fig. 6. A comparatively

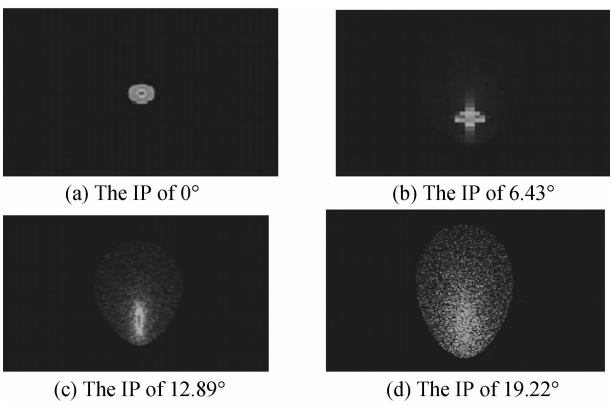

Fig. 6 The imaging result of the ommatidium with different incident angel

clear image point could take shape within 6°, and the image point turn to a cometary shape gradually with the increase of incident angle. So, as mentioned before, a separate ommatidium could only form a clear image point within a small angle.

Each ommatidium can be regarded as an independent imaging unit. Everyone formed a subimage in a small FOV and the co-property part came into being due to the overlapping of any two adjacent FOV. So, a complete image can be obtained by integrating the clear part of those subimages with the overlapping regions eliminated by confirming the arrangement characteristics and relation among those ommatidia[18].

2 Manufacturing process

As mentioned above, photoresist reflow method is suitable to manufact the multi-focusing ACE rapidly and at little cost. The manufacturing process consist of two major steps: the thermal reflow forming of planar ACE and the negative pressure forming of curved ACE.

Firstly, researchers spined the AZ4620 photoresist on the silicon substrate and formed a series of uniform cylinder structure by UV-lithography with the prepared mask. Here, researchers controlled the thickness of photoresist about 30 μm on account of the calculation above. Then, the substrate with cylinder structure was put in a constant temperature oven which is set to a suitable temperature for required time. The cylindrical structure formed a microlens array under the action of surface tension when the photoresist melted. With this, planar microlens array is achieved.

Afterwards, previous planar array was used as a template to fabricate a layer of PDMS membrane. Then the membrane was fixed on a vacuum drum and processed into a curved surface by negative pressure. After pouring the Norland81 into the structure accurately with a PDMS coelomic compartment, the membrane was exposed to UV light for 10 s. Finally, researchers obtained the curved multi-focusing ACE after demoulding.

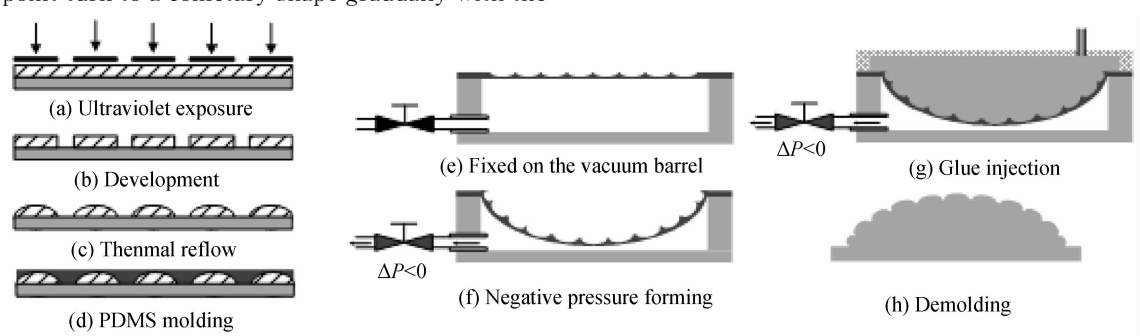

Fig. 7 The schematic diagram of manufacturing process

What calls for special attention is that the thickness of photoresist should be strictly controlled. If the coating photoresist can′t meet the minimum requirements, then it will make the center of the

spherical colloidal concave downward due to the effect of infiltration angle. On the other way, the nitrogen released by the diazo naphthoquinone will bring in the deformation problem during the exposure process if the thickness is over the limit.

As shown above, the dose of photoresist determines the shape of the ommatidium. Only the diameter of each unit on the photographic mask D_n and the thickness of photoresist H was used as the design variable. H depends on the spin speed of spin coater as shown in Fig. 8.

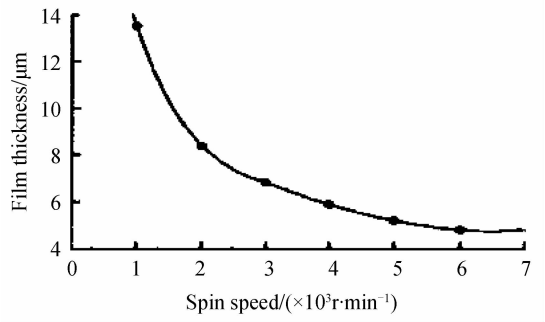

Fig. 8 The relationship between H and spin speed

Fig. 9 shows the diameters of seven rings of photographic mask under different thickness H. Synthesizes various factors, including production costs, extension of rings, and precision of mask and so on, the value of H was selected as 30 μm. In order to obtain the optimal $H\approx30$ μm, spin speed was chose to 800r/min and then the secondary spin was conducted.

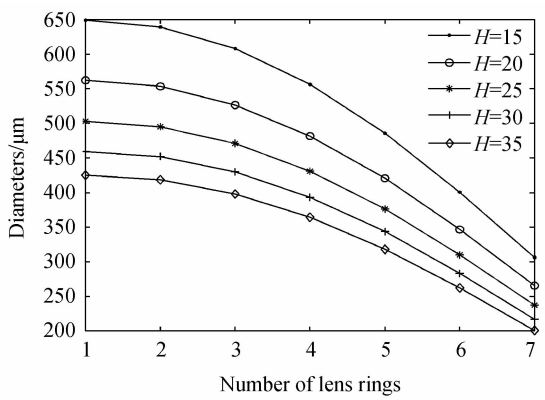

Fig. 9 The diameters under different H

Since the thickness H was fixed on the same substrate, the difference came from the diameter D_n. Fig. 10 shows that the measured data of ommatidia including the average height h_n and the curvature radius r_n are closed to the theoretical calculation. Also, it can be concluded that h_n and r_n increase with the increase of bottom diameter. Combining with the previous formula, focal length f_n increases as the same. Multi-focusing ACE with decreasing focal length was proven to be feasible. Also it shows that the height h_n should not be too large since the deficiency affected by central-dip, uneven glue and other factors.

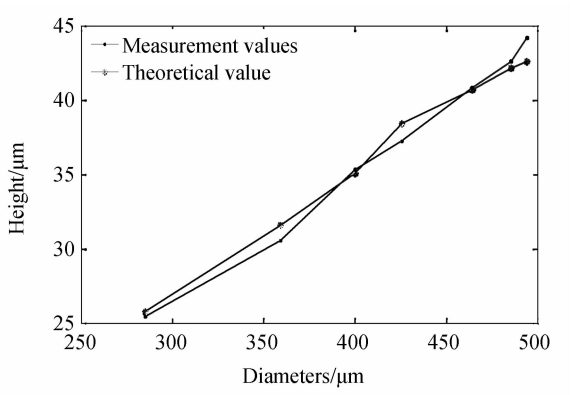

Fig. 10 The average height of ommatidia

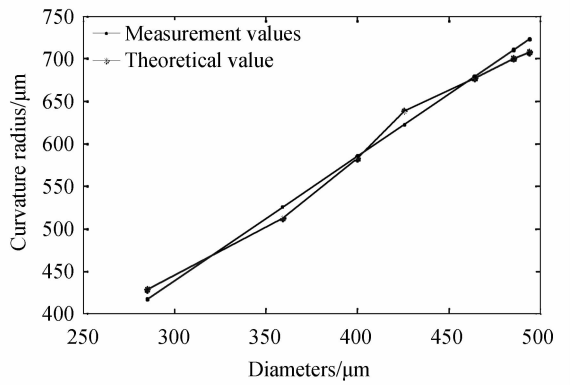

Fig. 11 The average curvature radius of ommatidia

During the process of glue injection, researchers bring in a PDMS cavity chamber to control the thickness of the base precisely and eliminate the influence of the air and impurities. Norland81 was chosen not only for its excellent optical performance, but for the extremely short exposure time which can protect the lithography equipment effectively.

3 Conclusion

The method of photoresist reflow, being the simplest method to fabricate microlens arrays at present, is the easiest means for mass production. Based on the method of photoresist reflow, this paper puts forward a new structure of curved bionic compound eyes. The ommatidia are arranged in the form of concentric circles and are of same aperture with a decreasing trend in aperture from the inside to the outside. The specific aperture can be obtained according to the calculations to ensure that each ommatidium can clearly imaging on a same focal plane during a certain angle range. Simulation using ZEMAX has proved the ACE′s function that even in the large field of view, clear image can be gained by corresponding ommatidium. Theoretically, increase in the amount of concentric circles may get the viewing angle of ACE to infinitely close to 180°. The initial ACE models we made has been proved certain defocus in imaging experiments, and the later improvement is

mainly aimed for compensating the impact that the changes of substrate curvature driving the aperture of ommatidium bring on the focus of each ommatidium while manufacturing curved lens. And by using the compensation dosage and redistributing the photoresist we can make improvements of the defocus of the ommatidia.

References

[1] ADELSON E H, WANG J YA. Single lens stereo with a plenoptic camera[C]. IEEE Transactions on Pattern Analysis and Machine Intelligence, 1992, **14**(2): 99-106.

[2] OGATA S, ISHIDA J, SASANO T, *et al*. Optical sensor array in an artificial compound eye [J]. *Optical Engineering*, 1994, **33**(11): 3649-3655.

[3] TANIDA J, KUMAGAI T, YAMADA K, *et al*. Thin observation module by bound optics (TOMBO): concept and experimental verification[J]. *Applied Optics*, 2001, **40**(11): 1806-1813.

[4] DUPARRE J, DANNBERG P, SCHREIBER P, *et al*. Artificial apposition compound eye fabricated by micro-optics technology[J]. *Applied Optics*, 2004, **43**(22): 4303-4310.

[5] DUPARRE J, SCHREIBER P, MATTHES A E, *et al*. Microoptical telescope compound eye[J]. *Optics Express*, 2005, **13**(3): 889-903.

[6] ZHANG Yu, LIU De-sen. Manufacture of hexagon aperture plane micro-lens array and its basic characteristics[J]. *Acta Photonica Sinaca*, 2008, **37**(8): 1639-1642.

[7] NG R, LEVOY M, BRéDIF M, *et al*. Light field photography with a hand-held plenoptic camera [J]. *Computer Science Technical Report CSTR*, 2005, **2**(11).

[8] DI Si, LIN Hui, DU Ru-xu, *et al*. An artificial compound eyes imaging system based on MEMS technology [C]. IEEE International Conference on Robotics and Biomimetics, 2009, 13-18.

[9] HORNSEY R, THOMAS P, WONG W, *et al*. Electronic compound-eye image sensor: construction and calibration[J]. *Electronic Imaging* 2004, 2004, 13-24.

[10] WIMMER R. FlyEye: grasp-sensitive surfaces using optical fiber[C]. Proceedings of the fourth international conference on Tangible, embedded, and embodied interaction, 2010, 245-248.

[11] KIM J, JEONG K H, LEE L, et al. Artificial ommatidia by self-aligned microlenses and waveguides[J]. *Optics Letters*, 2005, **30**(1): 5-7.

[12] LI Lei, YI A Y. Development of a 3D artificial compound eye [J]. *Optics Express*, 2010, **18**(17): 18125-18137.

[13] ZHANG Hao, LI Lei, McCray D L, *et al*. Development of a low cost high precision three-layer 3D artificial compound eye [J]. *Optics Express*, 2013, **21**(19): 22232-22245.

[14] JIN Jian, DI Si, YAO Yu-pei, *et al*. Design and fabrication of filtering artificial-compound-eye and its application in multispectral imaging [C]. ISPDI 2013-Fifth International Symposium on Photoelectronic Detection and Imaging, 2013, 891106.

[15] KEUM D, JEONG K H. Artificial compound eye with fractal zone plate arrays [C]. Optical MEMS and Nanophotonics (OMN) 2013 International Conference, 2013, 31-32.

[16] FLOREANO D, PERICET-CAMARA R, VIOLLET S, *et al*. Miniature curved artificial compound eyes [J]. *Proceedings of the National Academy of Sciences*, 2013, **110**(23): 9267-9272.

[17] GAO Tian-yuan, DONG Zheng-chao, ZHAO Yu, *et al*. Structure and alignment of field stitching compound eye optical imaging system[J]. *Acta Photonica Sinaca*, 2014, **43**(11): 1122001.

[18] CAO A-xiu, SHI Li-fang, SHI Rui-ying, *et al*. Image processing algorithm study of large fov compound eye structure [J]. *Acta Photonica Sinaca*, 2014, **43**(5): 0510005.

[19] XING Qiang, DAI Zhen-dong, WANG Hao. A rapid position estimation algorithm inspired of compound eyes [J]. *Acta Photonica Sinaca*, 2014, **43**(6): 0612001.

[20] DI Si, Du Ru-xu. Optimal design of single-layer spherical compound eye imaging system [J]. *Opto-Electronic Engineering*, 2010, **37**(2): 27-31.

[21] YANG Jun, JIANG Wei-tao, WANG Lan-lan, *et al*. Deformation analysis for curved compound eye in micro replica process[J]. *Journal of Xi'an Jiaotong University*, 2013, **47**(05): 121-125.